

## THE ABUNDANCE OF BULLET-GROUPS IN $\Lambda$ CDM

J. G. FERNÁNDEZ-TRINCADO<sup>1,2,3</sup>, J. E. FORERO-ROMERO<sup>1</sup>, G.FOEX<sup>4</sup>, T. VERDUGO<sup>3</sup> AND V. MOTTA<sup>4</sup>

<sup>1</sup> Departamento de Física, Universidad de los Andes, Cra. 1 No. 18A-10, Edificio Ip, Bogotá, Colombia

<sup>2</sup> Institute Utinam, CNRS UMR6213, Université de Franche-Comté, OSU THETA de Franche-Comté-Bourgogne, Besançon, France

<sup>3</sup> Centro de Investigaciones de Astronomía, AP 264, Mérida 5101-A, Venezuela

<sup>4</sup> Instituto de Física y Astronomía, Universidad de Valparaíso, Avda. Gran Bretaña 1111, Playa Ancha, Valparaíso 2360102, Chile

Submitted for publication in *ApJL*

### ABSTRACT

We estimate the expected distribution of displacements between the two dominant dark matter (DM) peaks (DM-DM displacements) and between DM and gaseous baryon peak (DM-gas displacements) in dark matter halos with masses larger than  $10^{13}h^{-1}M_{\odot}$ . We use as a benchmark the observation of SL2S J08544-0121, which is the lowest mass system ( $1.0 \times 10^{14}h^{-1}M_{\odot}$ ) observed so far featuring a bi-modal dark matter distribution with a dislocated gas component. We find that  $(50 \pm 10)\%$  of the dark matter halos with circular velocities in the range  $300 \text{ km s}^{-1}$  to  $700 \text{ km s}^{-1}$  (groups) show DM-DM displacements equal or larger than  $186 \pm 30h^{-1}\text{kpc}$  as observed in SL2S J08544-0121. For dark matter halos with circular velocities larger than  $700 \text{ km s}^{-1}$  (clusters) this fraction rises to  $(70 \pm 10)\%$ . Using the same simulation we estimate the DM-gas displacements and find that 0.1 to 1.0% of the groups should present separations equal or larger than  $87 \pm 14h^{-1}\text{kpc}$  corresponding to our observational benchmark; for clusters this fraction rises to  $(7 \pm 3)\%$ , consistent with previous studies of dark matter to baryon separations. Considering both constraints on the DM-DM and DM-gas displacements we find that the number density of groups similar to SL2S J08544-0121 is  $\sim 6.0 \times 10^{-7} \text{ Mpc}^{-3}$ , three times larger than the estimated value for clusters. These results open up the possibility for a new statistical test of  $\Lambda$ CDM by looking for DM-gas displacements in low mass clusters and groups.

*Subject headings:* dark matter — galaxies: clusters: individual (SL2S J08544-0121) — galaxies: interactions — methods: numerical

### 1. INTRODUCTION

The Bullet Cluster (1E0657—56) provided a new kind of observational evidence for the existence of dark matter (Markevitch et al. 2004; Clowe et al. 2006). Since then it has been used to test the Cold Dark Matter (CDM) paradigm itself by quantifying different aspects such as the expected displacement between the dominant dark matter and baryonic component in a  $\Lambda$ CDM Universe (Forero-Romero et al. 2010), the substructure velocity required to produce such displacement (Milosavljević et al. 2007; Springel & Farrar 2007; Mastropietro & Burkert 2008) and its abundance in large N-body cosmological simulations (Hayashi & White 2006; Lee & Baldi 2012; Thompson & Nagamine 2012). It has also been used to constrain the dark matter particle self-interaction cross section and to explore possible extensions to the concordance cosmological model (Farrar & Rosen 2007; Lee & Komatsu 2010).

Since then, other examples of Bullet-like systems have been found; MACS J0025.4-1222 (Bradač et al. 2008), Abell 2744 (Merten et al. 2011), DLSCL J0916.2+2951 (Dawson et al. 2012), ZwCl 1234.0+02916 (Dahle et al. 2013). Recently Gastaldello et al. (2014) observed a DM-gas displacement of  $87 \pm 14h^{-1}\text{kpc}$  and a DM-DM separation of  $186 \pm 30h^{-1}\text{kpc}$  in SL2S J08544-0121, a low mass cluster system with a total mass  $2.4 \pm 0.6 \times 10^{14}M_{\odot}$  found in the the Strong Lensing Legacy Survey (SL2S) sample (Cabanac et al. 2007; More et al. 2012).

Using a Sheth-Mo-Tormen mass function at  $z = 0$ , one

can estimate that systems around this mass are  $\sim 65$  times more abundant than massive clusters in the mass range of the Bullet Cluster  $> 10^{15}h^{-1}M_{\odot}$  (Sheth et al. 2001; Murray et al. 2013). This should open up the possibility of finding Bullet-like groups in large numbers to test  $\Lambda$ CDM. However, a larger abundance of small mass systems has to be weighted by the probability of being in a merger and presenting a large displacement between the DM and gaseous components. These two conditions (merger rates, maximum possible displacement) are a function of DM halo mass in  $\Lambda$ CDM cosmologies. A detailed statistical study to estimate the DM-gas displacements of bullets has been performed for clusters (Forero-Romero et al. 2010) but not for lower mass systems.

In this Letter we extend such study for systems in the group mass scale. We measure the abundance of DM systems with a multi-modal morphology (large DM-DM displacements) and estimate the amount of systems with a Bullet-like configuration (large DM-gas displacements). To this end we use a high resolution N-body cosmological simulation (Bolshoi) that allows us to find multi-modal dark matter distributions in hosts with circular velocities larger than  $300 \text{ km s}^{-1}$  ( $\sim 1.0 \times 10^{13}h^{-1}M_{\odot}$ ).

This Letter is organized as follows. In Section 2 we present the simulation and the halo catalogs. We continue in Section 3 with the geometry of the problem at hand and the measurement setup. Next in Section 4 we present our results and observational perspectives to finally conclude in Section 5.

### 2. SIMULATION, HALO CATALOGS AND PAIRS

We use the Bolshoi Run, a cosmological DM only simulation over a cubic volume of  $250h^{-1}\text{Mpc}$  comoving on a side (Klypin et al. 2011). The simulation uses the ART code (Kravtsov et al. 1997) to follow the evolution of a dark matter density field from  $z = 80$  to  $z = 0$  sampled with  $2048^3$  particles. The cosmology used corresponds to the spatially flat concordance model with the following parameters: the density parameter for matter (dark matter and baryons)  $\Omega_m = 0.27$ , the density parameter for baryonic matter  $\Omega_b = 0.0469$ , the density parameter for dark energy  $\Omega_\Lambda = 0.73$ , the Hubble parameter  $h = 0.7$ , the slope of the primordial power spectrum  $n = 0.95$  and the amplitude of mass density fluctuations (at redshift  $z=0$ )  $\sigma_8 = 0.82$ . These cosmological parameters are consistent with the nine-year Wilkinson Microwave Anisotropy Probe (WMAP) results (Hinshaw et al. 2013). A detailed presentation of the simulation can be found in Klypin et al. (2011).

This results in a mass resolution of  $1.35 \times 10^8 M_\odot h^{-1}$  for each computational particle. The completeness limit in this simulation is set for halos with 100 particles corresponding to a mass of  $1.35 \times 10^{10} h^{-1} M_\odot$  or a maximum circular velocity  $V_c$  of  $50 \text{ km s}^{-1}$ .

We use DM halo catalogs constructed using the Bound Density Maxima (BDM) algorithm (Klypin & Holtzman 1997; Klypin et al. 1999). To define the radius of a halo we use a density threshold of 360 times the mean density of the Universe. An important feature of BDM is that it allows us to detect sub-halos inside larger virialized structures.

All the raw data used in this Letter are available through the Multidark database <sup>1</sup> (Riebe et al. 2013). Furthermore, in order to facilitate the reproducibility and reuse of our results we have made available all the data and the source code available in a public repository <sup>2</sup>.

To construct our main halo sample we follow three steps. Firstly, we select all the host halos (i.e. halos that are not inside a larger halo) with circular velocities  $V_c \geq 300 \text{ km s}^{-1}$  ( $\geq 1 \times 10^{13} h^{-1} M_\odot$ ). Secondly, we select the sub-halos with circular velocities  $V_c \geq 75 \text{ km s}^{-1}$  ( $\geq 5 \times 10^{10} h^{-1} M_\odot$ ). Thirdly, we associate each host halo to its most massive sub-halo.

Each one of the pairs (host & sub-halo) is considered as a potential Bullet-like system and is kept for the analysis described in the next Section by using the sub-halos as the tracer of the sub-dominant dark matter clump in the merging cluster, i.e. the bullets.

Finally, we split the sample into two populations; groups, with  $300 \text{ km s}^{-1} < V_{c,\text{host}} < 700 \text{ km s}^{-1}$ ; and clusters, with  $V_{c,\text{host}} > 700 \text{ km s}^{-1}$  ( $\geq 8.0 \times 10^{13} h^{-1} M_\odot$ ). These two samples are constructed at four redshifts:  $z = 0.0, 0.25, 0.5$  and  $1.0$ . The number of pairs at each redshift in each population is listed on the first row of Table 1.

### 3. BULLET GEOMETRY AND MEASUREMENT SETUP

Bullet-like configurations have two dominant dark matter structures: the host halo and the dominant sub-halo. We describe the kinematics of this configuration

by the position and velocity vectors of the sub-halo in a frame of reference where the main halo is at rest; thus  $\vec{v} = \vec{v}_{\text{sub}} - \vec{v}_{\text{host}}$  and  $\vec{r} = \vec{r}_{\text{sub}} - \vec{r}_{\text{host}}$ , where the subscripts *host* and *sub* refer to the host and sub-halo, respectively. The positions  $\vec{r}$  correspond to the minimum of potential and the velocities  $\vec{v}$  are computed as an average of the bulk velocities of all simulation particles in the structure of interest.

The angle between these two vectors can be quantified by,

$$\mu \equiv \cos(\theta) = \frac{\vec{v} \cdot \vec{r}}{\|\vec{v}\| \|\vec{r}\|}. \quad (1)$$

This encodes information about the collision, i.e. cases of  $|\mu| \sim 1$  can be considered as head-on collisions while  $|\mu| < 0.9$  describes a grazing trajectory.

The geometrical configuration can be further described by the the circular velocity of each component and the size of the host halo  $R_{\text{vir}}$ . Another useful quantity computed in the simulation is the distance between the minimum of potential for the host halo and its center of mass (computed from all the particles inside the  $R_{\text{vir}}$ ),  $X_{\text{off}} = \|\vec{r}_{\text{min}} - \vec{r}_{\text{cm}}\|/R_{\text{vir}}$ , which serves as a measurement of how much the host halo is perturbed.

In this Letter we work with two quantities that could be inferred from observations of Bullet-like systems. The projected distance between two dominant DM clumps,  $d_{2D}$ , and the projected distance between the DM and the gas clumps,  $d_{2D}^{\text{bar}}$ . The projection is computed along the same axis for all halos at all redshifts, we present the result of the projection along the  $z$ -axis of the simulation.

From the simulation point of view, the first quantity can be translated into the 2D projected values of  $\|\vec{r}\|$  and its value relative to the virial radius  $D_{\text{off}} = \|\vec{r}\|_{2D}/R_{\text{vir}}$ . The second quantity, the projected DM-gas distance, is not directly available from a DM-only simulation but can be estimated from the data.

We also use the physical quantities described above to discriminate three main stages in a Bullet-like encounter with  $|\mu| \sim 1$ . First, when the sub-halo crosses the virial radius of the host halo starting a head on collision,  $D_{\text{off}} \sim 1$  and  $\mu \sim -1$ . Second, as the sub-halo crosses for the first time the center of the host halo  $D_{\text{off}} < 1.0$  and  $\mu \sim 1$ . Third, as the sub-halo reaches apogee and comes back to the center of the halo  $D_{\text{off}} < 1.0$  and  $\mu \sim -1$ .

## 4. RESULTS

### 4.1. DM-DM Displacements

Figure 1 presents the integrated probability distribution for the DM-DM displacements,  $d_{2D}$ . The left panel shows the displacement in physical units and the right panel as a fraction of the virial radius of the host halo. The panel with the projected 2D physical displacements also shows a vertical stripe with the estimated displacement for the bullet group reported by Gastaldello et al. (2014).

In the group sample we see that a fraction of 40% to 60% should present a displacement equal than the estimate for SL2S J08544-0121; in the cluster sample this fraction increases to 70%-80%. The uncertainties in this estimates are derived from the uncertainties in the displacement measurement for SL2S J08544-0121. This fraction is naturally higher in more massive systems because they are larger in size. Normalizing the displace-

<sup>1</sup> [www.multidark.org](http://www.multidark.org)

<sup>2</sup> [https://github.com/Fernandez-Trincado/Bullet\\_Groups-2014](https://github.com/Fernandez-Trincado/Bullet_Groups-2014)

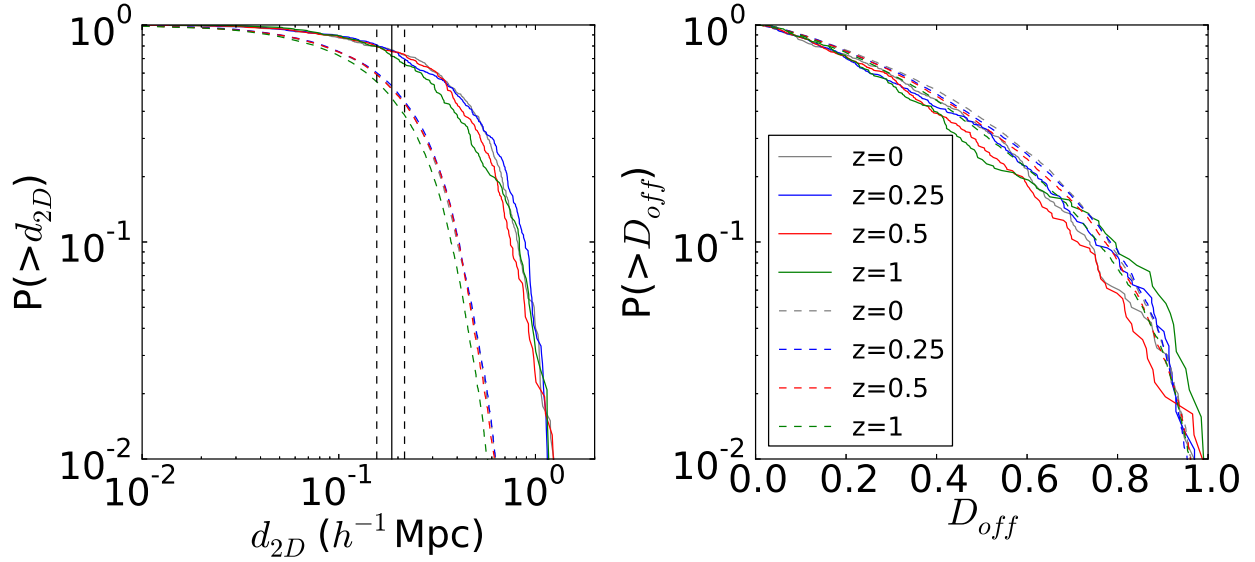


FIG. 1.— Integrated probability distribution for the displacement between the center of the host halo and its dominant sub-halo at all redshifts  $z = 0, 0.25, 0.5$  and  $1.0$ . The left panel shows the results in terms of the physical displacements while the right panel shows the displacements normalized by the virial radius of the host halo. The continuous (dashed) line corresponds to the halos in the cluster (group) sample. The vertical lines show the mean value and uncertainties ( $186 \pm 30 h^{-1} \text{kpc}$ ) in the separation between the two dark matter clumps estimated in Gastaldello et al. (2014) for the SL2S J08544-0121. Between 40% to 60% of the groups show a displacement equal or larger than this observational benchmark. This fraction rises to 60% and 80% in clusters.

ments by the virial radius, right panel Figure 1, we see that the distributions are similar for the two samples at all redshifts.

#### 4.2. Collision Geometries

Figure 2 presents the geometry of the interactions using the variables  $\mu$  and  $D_{\text{off}}$ . The first evident feature is that most of the configurations have head-on encounters,  $|\mu| > 0.9$  ( $\theta \leq 30^\circ$ ), while only a minority with  $|\mu| < 0.9$  can be described as having grazing trajectories.

For pairs on radial trajectories there are three regions of interest in this plane that correspond to the three merging stages described at the end of Section 4.2 assuming that the sub-halo merges (or falls below the BDM detection threshold) right at its second pass through the center of the host halo (Poole et al. 2006). These regions are shown as three different rectangles in Figure 2.

The first region has  $\mu < -0.9$  and  $D_{\text{off}} > 0.6$ , which locates the systems where a head-on collision has just started. The second region has  $\mu > 0.9$  and  $D_{\text{off}} < 0.6$ ; at this stage the collision continues after the first crossing of the host’s center. The low number of halos with radial infalling velocities and displacements  $D_{\text{off}} > 0.6$  suggests that this is the maximum range of radii for the apogee. The third region corresponds to  $\mu < -0.9$  and  $D_{\text{off}} < 0.6$  that is the secondary infall after apogee.

In the next subsection we use the information in this collision sequence to estimate the expected DM-gas displacement.

#### 4.3. DM-gas Displacements

The results we have derived so far apply to multi-modal systems and their expected separation between the two dominant dark matter clumps. However, a non-zero DM-DM displacement does not imply a non-zero DM-gas displacement. We now estimate these displacements from the available information in our DM only simulation.

Our estimates are based on the different kinds of trajectories and collision stages described in previous sections. To start with, we consider that systems with  $|\mu| < 0.9$  describing grazing trajectories have a DM-gas displacement equal to zero. In systems with head-on collisions,  $|\mu| > 0.9$  the systems with  $\mu < -0.9$  and large displacements  $D_{\text{off}} > 0.6$  most probably describe the beginning of the interaction and should have DM-gas displacements equal to zero as well. In all other cases the DM-gas displacement should be different from zero with the approximated value  $d_{2D}^{\text{bar}} = X_{\text{off}} R_{\text{vir}}$ , where  $X_{\text{off}}$  is the offset computed between the minimum of potential and the center of mass for each host halo computed from all the matter inside the virial radius.

This simplified model does not take into account that there is a fraction of halos with  $\mu < -0.9$  and  $D_{\text{off}} < 0.6$  for which the collision has not started and should have  $d_{2D}^{\text{bar}} = 0$ . A detailed modeling of this fraction requires the study of the complete merging history of the halo and sub-halo, a study beyond the scope of this Letter. Instead we caution the reader that the derived fraction of halos with a displacement  $< d_{2D}^{\text{bar}}$  must be considered as an upper limit.

The results for the integrated distributions for  $d_{2D}^{\text{bar}}$  are shown in Figure 3. The dashed lines represented the results for groups and the continuous lines correspond to clusters. As a test of our model we compare the cluster results against the analytic fit provided by Forero-Romero et al. (2010). This fit reproduces the statistics for the DM-baryon separation found for clusters more massive than  $> 10^{14} h^{-1} M_\odot$  in a simulation which included a description for DM and gas with 8 times more volume and 8 times less mass resolution than the Bolshoi Simulation. The fit is valid for separations larger than  $70 h^{-1} \text{kpc}$ , beyond which we find that it provides a remarkably good description within a factor of  $\sim 2$  of our results. This gives us confidence in our approach to

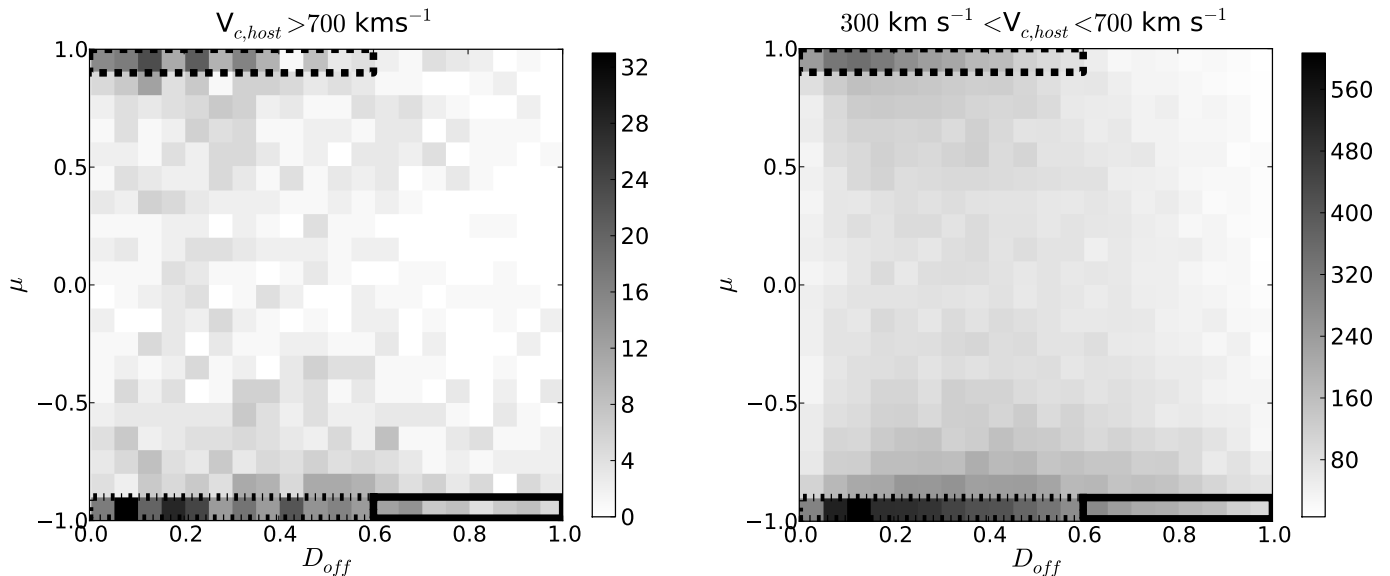


FIG. 2.— 2D histograms in the plane  $\mu$ - $D_{\text{off}}$  describing the geometry of the bullet encounter. The left panel corresponds to clusters and the right panel to groups. The weak redshift evolution of the structure in these planes allows us to include halos at all redshifts to construct these figures. The three rectangles (continuous, dashed, dashed-dotted) delimit stages of interest in a head-on collision as described in Section 4.2.

correctly estimate the expected fraction of groups with a DM-gas displacement.

Finally, from Figure 3 we see that only a fraction of 0.1% to 1% of the groups are expected to have a DM-gas displacement equal or larger than  $87 \pm 14 h^{-1} \text{kpc}$  as observed in SL2S J08544-0121. This fraction rises to 4% to 10% in the case of clusters, consistent with the results reported by Forero-Romero et al. (2010).

#### 4.4. Towards a Statistical Comparison Against Observations

Recently Foëx et al. (2013) presented an analysis of 80 galaxy groups in the SL2S sample. From the light distribution, only 34 objects ( $\sim 42\%$ ) have regular isophotes, 33 had elongated isophotes (hints of merging system), and 13 ( $\sim 16\%$ ) had a clear bi-modal light distribution; SL2S J08544-0121 is one of these 13 systems.

The bi-modal objects are defined to have at least a clear second luminosity peak within  $350 h^{-1} \text{kpc}$  from the main halo, as traced by the strong lensing system. The lowest separation in those systems is  $64 h^{-1} \text{kpc}$  and the average is  $145 \pm 52 h^{-1} \text{kpc}$ .

We now make a comparison of these fractions against the results of our simulations. The results are summarized in Table 1. The first row indicates the total number of halos in each sample at each redshift. The second row shows the number of objects with DM-DM displacements  $46 h^{-1} \text{kpc} < d_{2D} < 350 h^{-1} \text{kpc}$ . The last row indicates the number of objects in the previous sub-sample with DM-gas displacements  $d_{2D}^{\text{bar}} > 87 h^{-1} \text{kpc}$ .

Considering that the statistics for the cluster sample are dominated by objects in the mass range of the SL2S J08544-0121 we make a comparison against this sample. Table 1 shows that  $\sim 40\%$  of the clusters are expected to have large DM-DM displacements, which is a factor of  $\sim 2$  larger than the observational estimate by Foëx et al. (2013). However, roughly  $\sim 7\%$  of these systems present a displacement equal or larger than the observed in the SL2S J08544-0121, a fraction that is compatible

with the  $1/13 \sim 0.07$  fraction in the SL2S sample from which SL2S J08544-0121 was drawn.

This rough comparison shows that our estimates for the relative number of bullet systems (large DM-gas displacements) with respect to multi-modal systems (large DM-DM displacements) is compatible with observations. A proper comparison must take into account all the observational uncertainties, biases and mixes between our two populations (groups & clusters at different redshifts) to derive a stronger bound from the simulation, something that is beyond the scope of this Letter.

Nevertheless, comparing the absolute number of systems with characteristics similar to SL2S J08544-0121 in the group sample (last row of Table 1) we predict that its number density is  $\sim 6.0 \times 10^{-7} \text{Mpc}^{-3}$ , three times larger than the expected number density of SL2S J08544-0121 systems in the cluster sample.

## 5. CONCLUSIONS

In this Letter we estimated the fraction of galaxy groups and clusters in a  $\Lambda$ CDM cosmology that could present observational features associated to a Bullet-like event. This is motivated by the recent observational results of Gastaldello et al. (2014) where a system (SL2S J08544-0121) on the mass range  $1 \times 10^{14} h^{-1} M_{\odot}$  and velocity dispersion  $650 \text{ km s}^{-1}$  was reported to feature a displacement between its baryonic (gas) and dark matter components.

We computed the distribution of projected displacements between the dominant DM clumps in two kinds of systems; groups with circular velocities  $300 \text{ km s}^{-1} < V_c < 700 \text{ km s}^{-1}$  ( $1.0 \times 10^{13} h^{-1} M_{\odot} < M_{\text{vir}} < 8.0 \times 10^{13} h^{-1} M_{\odot}$ ) and clusters with  $V_c > 700 \text{ km s}^{-1}$  ( $M_{\text{vir}} > 8.0 \times 10^{13} h^{-1} M_{\odot}$ ). We reported these results at four different redshifts  $z = 0.0, 0.25, 0.5$  and  $1$ . Our results are based on large DM-only N-body cosmological simulation with a resolution that allows us to study for the first time Bullet-like configurations in the mass range of

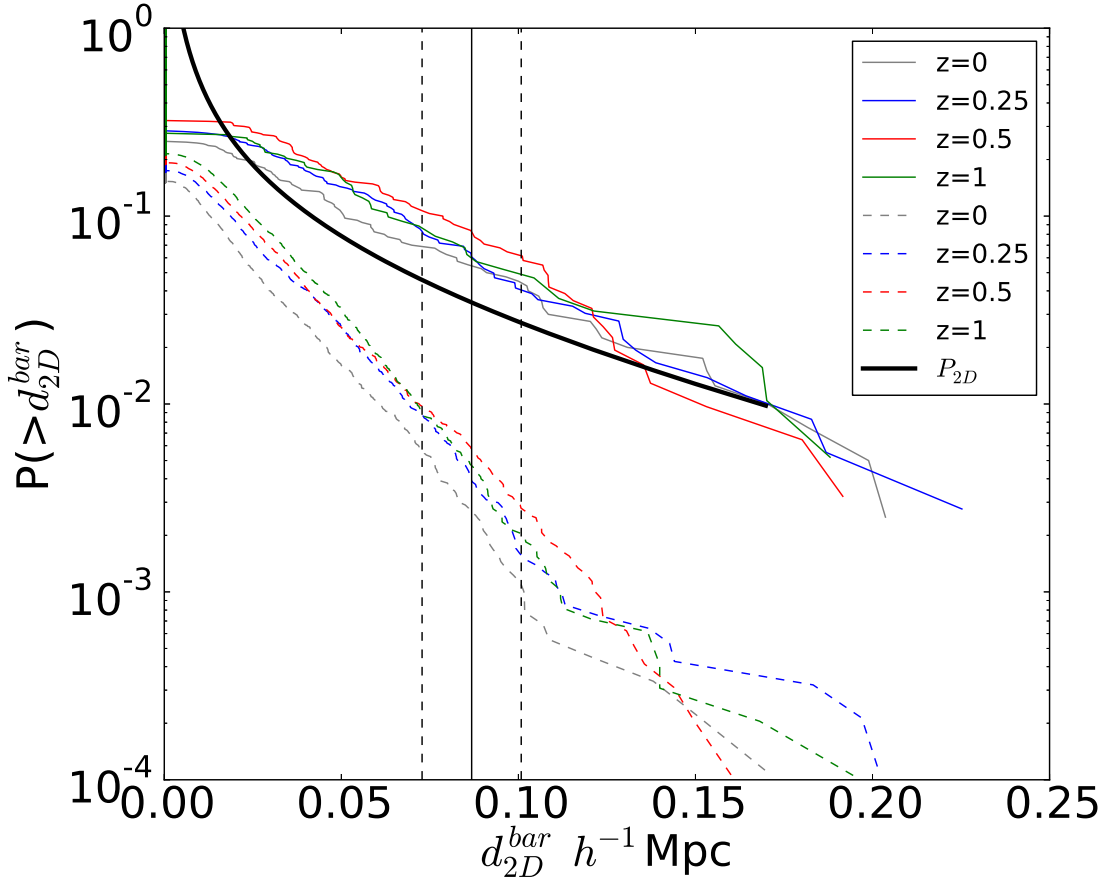


FIG. 3.— Integrated probability distribution for the estimated DM-gas displacements in the group and cluster samples. Continuous (dashed) lines correspond to clusters (groups). The continuous black line marked as  $P_{2D}$  shows the statistics reported by Forero-Romero et al. (2010) for a cosmological simulation including DM and gas. The vertical lines correspond to the mean value and uncertainty of the displacement measured for SL2S J08544-0121.

	Groups $z = 0$ (#)	Groups $z = 0.25$ (#)	Groups $z = 0.5$ (#)	Groups $z = 1.0$ (#)	Clusters $z = 0$ (#)	Clusters $z = 0.25$ (#)	Clusters $z = 0.5$ (#)	Clusters $z = 1.0$ (#)
Full Sample	9641	9984	10244	10190	400	363	310	192
$64 < d_{2D}/h^{-1}\text{kpc} < 350$	6188	6422	6635	6933	151	141	120	99
$(64 < d_{2D}/h^{-1}\text{kpc} < 350) \ \& \ (d_{2D}^{\text{bar}}/h^{-1}\text{kpc} > 87)$	14	25	44	35	8	9	13	8

TABLE 1

ABSOLUTE NUMBER OF OBJECTS IN THE GROUPS AND CLUSTERS SAMPLE AT ALL REDSHIFTS FOR DIFFERENT SELECTION CRITERIA.

galaxy groups.

Our main result is that a fraction of 40%-60% of the halos in the group sample presents DM-DM displacement equal or larger than the observed displacement for SL2S J08544-0121. For halos in the cluster sample this fraction increases to 60%-80%. We also derived an estimate for the DM-baryon displacement. In the group sample 0.1%-1.0% of the halos show a displacement equal or larger than the measurements of SL2S J08544-0121 by Gastaldello et al. (2014); in the cluster sample this fraction rises to 4%-10%.

For the case of SL2S J08544-0121 a fair comparison is achieved against our cluster sample which has statistics dominated by objects of similar mass. In a rough comparison using the observational criteria (Foëx et al. 2013; Gastaldello et al. 2014) we find that the relative number of Bullet-like systems (large DM-gas displacement) with

respect to a general sample of multi-modal systems (large DM-DM displacements) is consistent with observations; both are in the range  $\sim 7\%$ .

Using the same criteria we find that in the simulation there are  $\sim 6.0 \times 10^{-7} \text{ Mpc}^{-3}$  groups similar to SL2S J08544-0121. This number density is three times larger than the computed value for clusters. This opens up a new observational possibility with surveys such as SL2S that target a large number of groups and estimate its multi-modal nature from lensing analysis (Foëx et al. 2013). An approach that can be further exploited with upcoming lensing surveys (e.g. with the *Euclid* satellite) and pushes for X-ray surveys with higher sensibility: chances are larger to find bullets in systems with lower X-ray luminosities.

We thank the referee for a detailed report that im-

proved the readability of this Letter.

The CosmoSim database used in this paper is a service by the Leibniz-Institute for Astrophysics Potsdam (AIP). The Bolshoi simulation was performed within the Bolshoi project of the University of California High-Performance AstroComputing Center (UC-HIPACC) and was run at the NASA Ames Research Center.

J.G.F-T acknowledges support from Universidad de los Andes de Bogotá - Colombia and Centro de Investigaciones de Astronomía (CIDA) - Venezuela.

J.E.F-R acknowledges support from Vicerrectoría de

Investigaciones through a FAPA starting grant.

G.F. acknowledges support from FONDECYT through grant 3120160 and ECOS/CONICYT through grant C12U02.

T.V. acknowledges support from CONACYT through grant 165365 and 203489 through the program Estancias posdoctorales y sabáticas al extranjero para la consolidación de grupos de investigación.

V.M. gratefully acknowledges FONDECYT support through grant 1120741 and ECOS/CONICYT through

## REFERENCES

- Bradač, M., Allen, S. W., Treu, T., Ebeling, H., Massey, R., Morris, R. G., von der Linden, A., & Applegate, D. 2008, *ApJ*, 687, 959
- Cabanac, R. A., Alard, C., Dantel-Fort, M., Fort, B., Gavazzi, R., Gomez, P., Kneib, J. P., Le Fèvre, O., Mellier, Y., Pello, R., Soucail, G., Sygnet, J. F., & Valls-Gabaud, D. 2007, *A&A*, 461, 813
- Clowe, D., Bradač, M., Gonzalez, A. H., Markevitch, M., Randall, S. W., Jones, C., & Zaritsky, D. 2006, *ApJ*, 648, L109
- Dahle, H., Sarazin, C. L., Lopez, L. A., Kouveliotou, C., Patel, S. K., Rol, E., van der Horst, A. J., Fynbo, J., Wijers, R. A. M. J., Burrows, D. N., Gehrels, N., Grupe, D., Ramirez-Ruiz, E., & Michałowski, M. J. 2013, *ApJ*, 772, 23
- Dawson, W. A., Wittman, D., Jee, M. J., Gee, P., Hughes, J. P., Tyson, J. A., Schmidt, S., Thorman, P., Bradač, M., Miyazaki, S., Lemaux, B., Utsumi, Y., & Margoniner, V. E. 2012, *ApJ*, 747, L42
- Farrar, G. R., & Rosen, R. A. 2007, *Physical Review Letters*, 98, 171302
- Foëx, G., Motta, V., Limousin, M., Verdugo, T., More, A., Cabanac, R., Gavazzi, R., & Muñoz, R. P. 2013, *A&A*, 559, A105
- Forero-Romero, J. E., Gottlöber, S., & Yepes, G. 2010, *ApJ*, 725, 598
- Gastaldello, F., Limousin, M., Foëx, G., Muñoz, R., Verdugo, T., Motta, V., More, A., Cabanac, R., Buote, D., Eckert, D., Ettori, S., Fritz, A., Ghizzardi, S., Humphrey, P., Meneghetti, M., & Rossetti, M. 2014, *MNRAS* accepted
- Hayashi, E., & White, S. D. M. 2006, *MNRAS*, 370, L38
- Hinshaw, G., Larson, D., Komatsu, E., Spergel, D. N., Bennett, C. L., Dunkley, J., Nolte, M. R., Halpern, M., Hill, R. S., Odegard, N., Page, L., Smith, K. M., Weiland, J. L., Gold, B., Jarosik, N., Kogut, A., Limon, M., Meyer, S. S., Tucker, G. S., Wollack, E., & Wright, E. L. 2013, *ApJS*, 208, 19
- Klypin, A., Gottlöber, S., Kravtsov, A. V., & Khokhlov, A. M. 1999, *ApJ*, 516, 530
- Klypin, A., & Holtzman, J. 1997, *ArXiv Astrophysics e-prints*
- Klypin, A. A., Trujillo-Gomez, S., & Primack, J. 2011, *ApJ*, 740, 102
- Kravtsov, A. V., Klypin, A. A., & Khokhlov, A. M. 1997, *ApJS*, 111, 73
- Lee, J., & Baldi, M. 2012, *ApJ*, 747, 45
- Lee, J., & Komatsu, E. 2010, *ApJ*, 718, 60
- Markevitch, M., Gonzalez, A. H., Clowe, D., Vikhlinin, A., Forman, W., Jones, C., Murray, S., & Tucker, W. 2004, *ApJ*, 606, 819
- Mastropietro, C., & Burkert, A. 2008, *MNRAS*, 389, 967
- Merten, J., Coe, D., Dupke, R., Massey, R., Zitrin, A., Cypriano, E. S., Okabe, N., Frye, B., Braglia, F. G., Jiménez-Teja, Y., Benítez, N., Broadhurst, T., Rhodes, J., Meneghetti, M., Moustakas, L. A., Sodré, Jr., L., Krick, J., & Bregman, J. N. 2011, *MNRAS*, 417, 333
- Milosavljević, M., Koda, J., Nagai, D., Nakar, E., & Shapiro, P. R. 2007, *ApJ*, 661, L131
- More, A., Cabanac, R., More, S., Alard, C., Limousin, M., Kneib, J.-P., Gavazzi, R., & Motta, V. 2012, *ApJ*, 749, 38
- Murray, S. G., Power, C., & Robotham, A. S. G. 2013, *Astronomy and Computing*, 3, 23
- Poole, G. B., Fardal, M. A., Babul, A., McCarthy, I. G., Quinn, T., & Wadsley, J. 2006, *MNRAS*, 373, 881
- Riebe, K., Partl, A. M., Enke, H., Forero-Romero, J., Gottlöber, S., Klypin, A., Lemson, G., Prada, F., Primack, J. R., Steinmetz, M., & Turchaninov, V. 2013, *Astronomische Nachrichten*, 334, 691
- Sheth, R. K., Mo, H. J., & Tormen, G. 2001, *MNRAS*, 323, 1
- Springel, V., & Farrar, G. R. 2007, *MNRAS*, 380, 911
- Thompson, R., & Nagamine, K. 2012, *MNRAS*, 419, 3560